Low-temperature (<450 °C), plasma-assisted deposition of poly-Si thin films on SiO_2 and glass through interface engineering

D. M. Wolfe, F. Wang, and G. Lucovsky[a)]
Departments of Materials Science and Engineering, Physics, and Electrical and Computer Engineering, North Carolina State University, Raleigh, North Carolina 27695

(Received 15 October 1996; accepted 11 March 1997)

A low-temperature, two-stage process that employs interface engineering is investigated for deposition of poly-Si thin films on SiO_2 and glass. In this two-stage process, film growth is separated into two regimes: (i) interface formation and (ii) bulk film growth. Interface formation (stage 1) was optimized for remote plasma enhanced chemical-vapor deposition (PECVD) of ultra thin (<100 Å) μc-Si films on the oxide. This layer acts as a seed template, providing ordered growth sites for the next stage of film growth. Bulk Si film deposition (stage 2) was then initiated on the seed template using remote PECVD process conditions shown to produce low-temperature (<450 °C), epitaxial-Si films on crystalline silicon substrates, so as to drive a transition to larger grain growth off of the seed crystals. Results showed that the seed layer had a dramatic impact on bulk film crystallinity. Films deposited without a μc-Si seed layer were amorphous, whereas films deposited using a seed layer, in conjunction with the appropriate second stage conditions, were highly oriented (220) poly-Si. © *1997 American Vacuum Society.* [S0734-2101(97)09703-0]

I. INTRODUCTION

Polycrystalline-Si (poly-Si) thin film deposition on SiO_2 and glass continues to receive considerable attention due to its widespread use in various microelectronic devices. Several studies have identified the possibility of forming poly-Si at reduced temperatures by using an interfacial ''seed layer'' approach. For example, Heath *et al.* used Si nanocrystals produced by excimer laser photolysis of disilane as seed nuclei prior to bulk film deposition.[1] Tanikawa and Tatsumi reported using a plasma seeding technique carried out using a nude ion gauge in a disilane atmosphere.[2] Matsumoto *et al.* utilized ⟨111⟩ oriented ZnS buffer layers, grown using diethyl zinc (DEZ) and H_2S precursors, before initiating bulk film growth.[3]

Using a similar approach, this study reports on low-temperature poly-Si thin film deposition through interface engineering, or two-stage processing. The foundational basis for this interface engineering approach is derived from consideration that as deposition temperature decreases, crystallization becomes difficult during the initial stages of film growth due to poor surface mobility of adatoms and the lack of ordered sites found on the starting amorphous oxide surface. To overcome this, our method is based on separating interface formation from bulk film growth by employing two processing steps. The first step, stage 1, was optimized for remote plasma enhanced chemical-vapor deposition (PECVD) of ultrathin (<100 Å) microcrystalline-Si (μc-Si) films. This seed layer acts as a template, providing ordered growth sites for the next stage of film deposition. For bulk film growth, stage 2, two sets of process conditions were optimized for low-temperature (<450 °C), remote PECVD of epitaxial-Si (epi-Si) films onto crystalline-Si substrates, so as to drive a transition to larger grain growth off of the seed crystals. Figure 1 is a schematic of the two-stage film structure.

Microcrystalline-Si film growth was tracked *in vacuo* using Auger electron spectroscopy (AES) and *ex situ*, with spectroscopic ellipsometry (SE) and reflection high energy electron diffraction (RHEED). Unannealed bulk Si films were analyzed for crystallinity using a combination of RHEED, x-ray diffraction (XRD), cross-sectional transmission electron microscopy (XTEM) and Raman spectroscopy. Results indicated that when no μc-Si template was used, the microstructure of films deposited directly on the oxide, with two different sets of optimized epi-Si deposition conditions, was amorphous. However, when a seed template was first deposited, the microstructure was found to be poly-Si for one set of epi-Si conditions and amorphous for the other, leading to the conclusion that both interface formation and choice of the second stage process conditions play a crucial role in determining the bulk film microstructure.

II. EXPERIMENTAL PROCEDURE

All films analyzed for this study, except those for Raman analysis, were deposited on 80 Å thick SiO_2 grown at 900 °C by dry oxidation on p-Si (100) wafers. Films to be used for Raman analysis were deposited on glass substrates (Corning 7059) in order to eliminate the possibility of a crystalline-Si substrate peak in the spectra.

Both stages of film deposition took place in the same chamber of an integrated ultrahigh vacuum (UHV) cluster tool system via remote PECVD, as described elsewhere.[4] Prior to sample insertion into the loadlock of the system, a 10 sec rinse in de-ionized water followed by a nitrogen gas dry was performed on the oxidized wafers. A 10 min ultrasonic bath in a sulfuric/chromic acid glass cleaning solution followed by a 10 min rinse in de-ionized water and nitrogen

[a)]Author to whom all correspondence should be addressed; Electronic mail: gerry_lucovsky@ncsu.edu

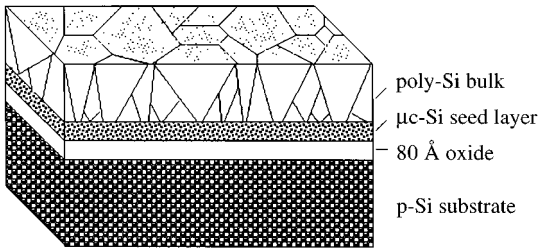

FIG. 1. Schematic of two-stage film structure. A thin μc-Si seed layer is deposited prior to bulk Si film deposition.

gas dry was done on the Corning 7059 substrates. Processing conditions for obtaining ultrathin μc-Si films on oxide and epi-Si films on crystalline Si substrates are summarized in Table I. Note that two different sets of epi-Si deposition conditions were used. To study the initial stages of μc-Si film growth, a series of films ranging from approximately 5 to 80 Å was deposited on SiO_2. Using *in vacuo* AES, the decay of the oxygen *KLL* substrate signal due to overlayer growth was analyzed for various film thicknesses to ascertain the growth mechanism of the film. To assess the crystallinity of the seed layer, *ex situ* RHEED and SE were employed. Prior to RHEED imaging, the native oxide was stripped using a dilute HF solution. Grazing angle ($\sim$3°) diffraction images were obtained at 10 keV accelerating voltage. For SE measurements, the shift in optical phase and the polarization upon reflection at 75° from the surface normal were analyzed utilizing a detector operating in the 1.6–3.0 eV spectral range.

Bulk film microstructural characterization was also done with RHEED, using the same conditions as above, along with XRD, XTEM and Raman spectroscopy. X-ray diffraction patterns were obtained using 1.5406 Å Cu $K\alpha_1$ radiation. The c-Si (400) reflection was used as alignment reference. Cross-sectional TEM imaging was performed in the bright-field mode at 200 keV beam voltage. For Raman analysis, an Ar^+ laser operating at 514.53 nm was used for excitation. Incident laser power on the sample was approximately 150 mW. Characterization was performed on films grown with and without various seed layer thicknesses using both sets of epi-Si deposition conditions, as listed in Table I.

TABLE I. Process parameters for obtaining μc-Si and epi-Si films by remote PECVD.

Stage 1: μc-Si seed layer template	
T=250 °C	p=300 mTorr
Upstream:	He—150 sccm, 50 W rf
Downstream:	SiH_4(10%/He)—10 sccm
	H_2—50 sccm
Stage 2: epi-Si bulk film deposition	
Conditions ''A''	
T=450 °C	p=50 mTorr
Upstream:	He—150 sccm, 50 W rf
Downstream:	SiH_4(10%/He)—10 sccm
	H_2—25 sccm
Conditions ''B''	
T=400 °C	p=500 mTorr
Upstream:	He—150 sccm, 50 W rf
Downstream:	SiH_4(10%/He)—10 sccm
	H_2—25 sccm

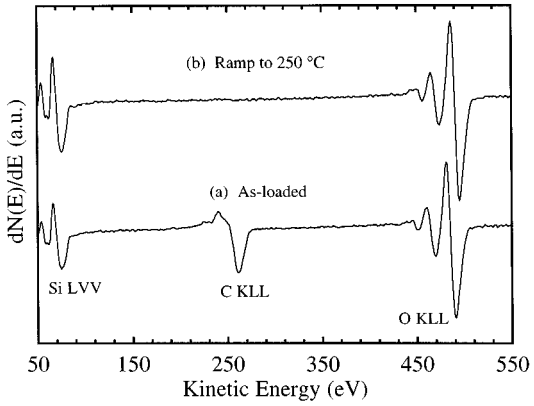

FIG. 2. AES of SiO_2 (a) before and (b) after ramping to 250 °C.

III. RESULTS AND DISCUSSION

A. Ultra-thin μc-Si film deposition

The SiO_2 starting surface was measured by AES before and after ramping to the process temperature for stage 1 μc-Si film growth, and is shown in Fig. 2. Carbon contamination is no longer detectable on the oxide after ramping to 250 °C. Consequently, it is deduced that carbon containing molecules are physiosorbed on the oxide surface, and therefore desorb at relatively low temperatures (<250 °C). Hence, a complex wet chemical pre-clean was not used, and only a 10 sec rinse in de-ionized water followed by a nitrogen gas dry was deemed necessary to remove any gross particulates from the surface.

Figure 3 shows the attenuated derivative O *KLL* signal normalized to an uncovered SiO_2 surface and plotted versus time (thickness) for the initial stages of film growth. Each point represents the average of 20 scans. The typical raw spectra are shown in the inset, with I_O being the unattenuated

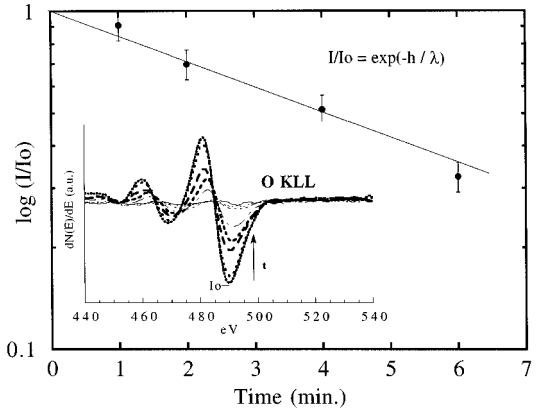

FIG. 3. Normalized AES oxygen *KLL* signal for the initial stages of μc-Si film growth on SiO_2. Inset shows the raw data.

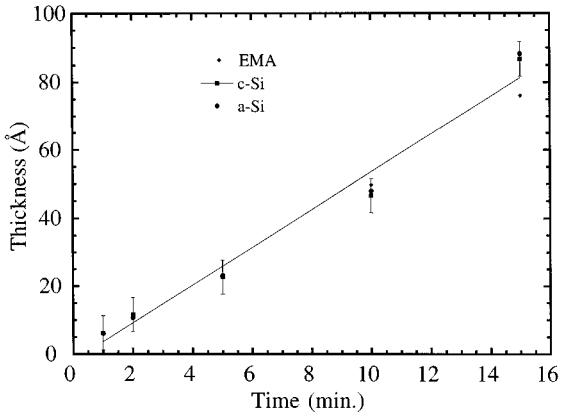

FIG. 4. Thickness vs time for the initial stages of μc-Si film growth on SiO_2 as determined via SE.

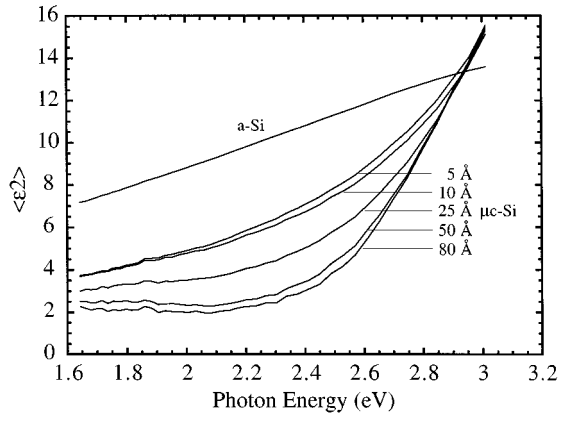

FIG. 5. Imaginary part of the pseudodielectric function vs photon energy for the initial stages of μc-Si film grown on SiO_2. An a-Si film is shown for comparison.

derivative O *KLL* signal intensity of the bare SiO_2 surface, and the arrow showing the trend of decreasing signal as film thickness increases. Signal decay in this growth regime is observed to follow the equation

$$\frac{I}{I_O} = \exp^{-h/\lambda} \tag{1}$$

where h is the overlayer film thickness and λ is the escape depth of the Auger O *KLL* electrons, which is approximately 10 Å.[5] Analysis of this trend suggests that film growth proceeds in a layer mechanism mode. Assuming that the escape depth of AES electrons from the oxide is constant, if film growth follows Eq. (1), then overlayer growth should occur in a uniform lateral manner, with complete layer formation occurring before the next layer is deposited; otherwise the slope of the plot in Fig. 3 would change with time.

Thickness measurements performed on these films using SE are shown in Fig. 4. A crystalline-Si (c-Si), amorphous-Si (a-Si), and Bruggeman effective medium approximation (EMA), which assumes isotropic mixtures of c-Si and a-Si, were compared for use as input optical models for calculating thicknesses from the data. Consistent with AES measurements, as film growth proceeds, thickness is observed to increase linearly in time, with approximately 5 Å/min of film deposition. Note that the thicknesses derived are relatively insensitive to the optical model used, particularly below 25 Å. Consequently, quantitative analysis of the microstructure, i.e., percent of crystalline fraction, voids, roughness, etc., was not evaluated.

Indirect assessment of film crystallinity was determined through $\langle \varepsilon_2 \rangle$ spectra, as shown in Fig. 5. Spectra were obtained for various μc-Si film thicknesses, with an amorphous silicon film shown for comparison. No optical model is assumed in these measurements, and $\langle \varepsilon_2 \rangle$ spectra are calculated directly from the imaginary part of the equation:[6]

$$\langle \varepsilon \rangle = \sin^2 \phi_0 + \sin^2 \phi_0 \tan^2 \phi_0 \left[\frac{1-\rho}{1+\rho}\right]^2, \tag{2}$$

where ϕ_0 is the angle of incidence (75 °) and ρ is the complex reflection coefficient, given by

$$\rho = \tan(\Psi)\exp(i\Delta) \tag{3}$$

in which Ψ, the amplitude change, and Δ, the phase change between the s and p components of polarization upon reflection are measured. For increasing film thicknesses, the $\langle \varepsilon_2 \rangle$ spectra are found to shift to lower values and clearly have a different curvature than that of the a-Si film. Consideration that the a-Si film used as reference shows higher absorption over that of the μc-Si films in the spectral range studied suggests that μc-Si film growth does begin with some crystalline material at or near the oxide surface. Hence, the spectra for the initial stages of film growth, as compared to that of the a-Si, are shifted to lower values due to the lower absorption coefficient of the c-Si phase present in the film. Also, from this shift towards lower values, crystallinity is believed to increase as film growth progresses.

For direct qualitative assessment of *surface* crystallinity in the ultrathin μc-Si films, RHEED imaging was used. Figure 6 shows a typical RHEED image obtained for an 80 Å μc-Si film deposited on SiO_2. The continuous ring structure is characteristic of a fine-grained (crystallite size ~100 Å) film, confirming the presence of crystalline seeds at the surface of the film, on which the next stage of deposition, stage 2, will begin. The (111), (220), and (311) reflections, as indexed by their relative distances from the primary beam, are present. The existence of only low-index growth planes in

FIG. 6. RHEED image of an 80 Å μc-Si film on SiO_2.

these ultrathin films, particularly the {111} planes, can be expected based on surface free energy considerations. A more detailed explanation would also include the effects of surface kinetics, the microscopic geometry of the growing surface, etc., and these are reviewed by Kakinuma.[7] Using Wulff's theorem,[8] the equilibrium crystal shape is given by γ_i/h_i = constant, where γ_i is the surface free energy of the ith plane and h_i is the perpendicular distance from the Wulff net origin to the plane. Use of this theorem for the low-index planes yields

$$\gamma_{111}/h_{111}=\gamma_{220}/h_{220}=\gamma_{311}/h_{311}=\text{const.} \quad (4)$$

Assuming the {111} planes have the lowest surface energy, h_{111} must be the lowest to satisfy Eq. (4). Therefore the {111} planes consume the largest part of the crystal surface and can be expected to form frequently during the initial stages of growth. Also note that plasma surface etching may be occurring during film growth and the existence of certain planes could be due to a higher resistance to etching. An identical image to that in Fig. 6 was obtained for 50 Å μc-Si films, however no ring structured could be differentiated from the background for thinner films. The influence of seed layer thickness on bulk film crystallinity will be discussed further in Sec. III B.

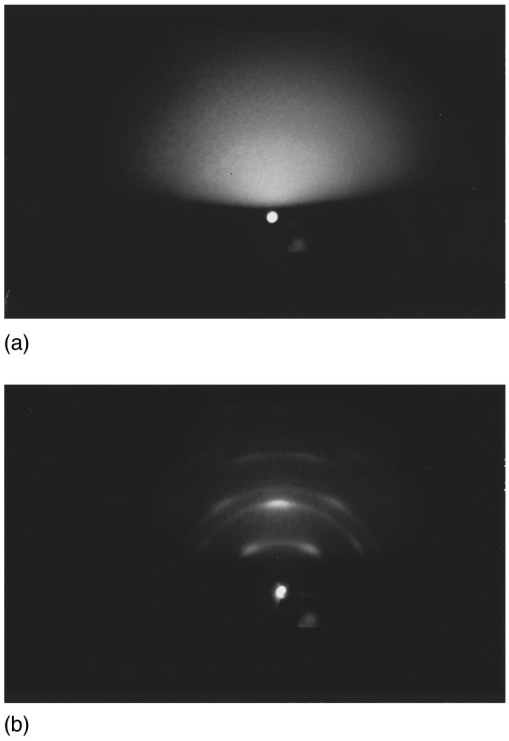

FIG. 7. RHEED images of 2000 Å films deposited on SiO_2 using epi-Si conditions ''A:'' (a) without a μc-Si seed layer (amorphous) and (b) with an 80 Å μc-Si seed layer (polycrystalline).

B. Two-stage processing

An 80 Å μc-Si film was chosen as the starting seed layer template for investigating the two-stage deposition process. This thickness was chosen because RHEED images unambiguously confirmed a starting μc-Si surface. The transition from stage one to stage two was discontinuous, meaning that reactant gas flow was stopped after deposition of the seed layer, the conditions for stage two growth obtained (ramp to temperature and pressure for epi-Si conditions), and then appropriate reactant gas flow reintroduced. The dramatic impact that the seed layer has on stage-two bulk film crystallinity is illustrated by RHEED images in Fig. 7. The images are for 2000 Å films deposited using epi-Si conditions ''A'' (see Table I) *without* a seed template (Fig. 7a); and *with* a seed template (Fig. 7b). Most notable is that when no seed template is used; films deposited directly on the oxide surface using optimized epi-Si conditions ''A'' are amorphous (Fig. 7a), with no sign of ordered ring formation. However, when a seed layer is first deposited, a distinct ring structure is formed (Fig. 7b) with high intensity maxima, indicative of poly-Si formation. Note that all reflections are present, with a strong maximum at the (220) zone center.

In contrast, films deposited using optimized epi-Si conditions ''B'' were found to be amorphous, regardless of whether or not a seed layer template was used. Images identical to Fig. 7a were produced in both cases. Figures 8a and 8b shows the Raman spectra for 2000 Å films deposited on an 80 Å μc-Si seed template using epi-Si conditions ''A'' and epi-Si conditions ''B,'' respectively. As illustrated, only the spectrum obtained from two-stage processed films utilizing epi-Si conditions ''A'' show the characteristic[9] crystalline 520 cm^{-1} optical phonon vibration mode, whereas films processed with epi-Si conditions ''B'' show no distinct crystalline vibration peak, only the broad 480 cm^{-1} amorphous feature. This key observation implies that deposition of a seed layer prior to bulk film growth does not guarantee crystalline formation in the second stage film. Even though both sets of deposition conditions produced high quality homoepitaxial films, one set is conducive for crystalline growth on the μc-Si template layer, the other is not. Futher work is needed to understand this behavior.

Now after establishing the optimum second stage epi-Si conditions (conditions ''A''), the influence of seed layer

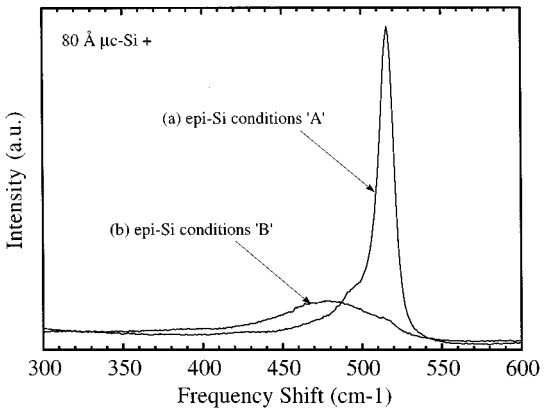

FIG. 8. Raman spectra of two-stage processed films with an 80 Å μc-Si seed layer and (a) epi-Si conditions ''A'' and (b) epi-Si conditions ''B'' bulk Si films.

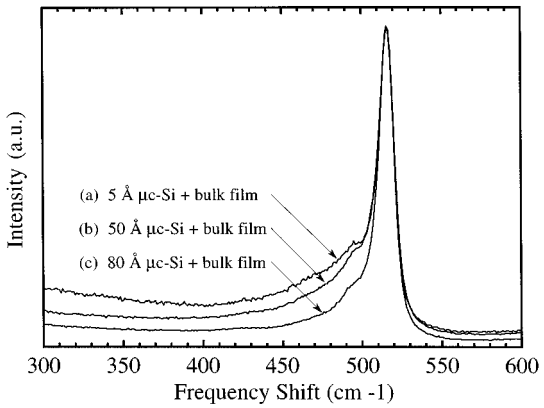

FIG. 9. Raman spectra of two-stage processed films with various μc-Si seed layer thicknesses. Bulk Si films were deposited using epi-Si conditions ''A.''

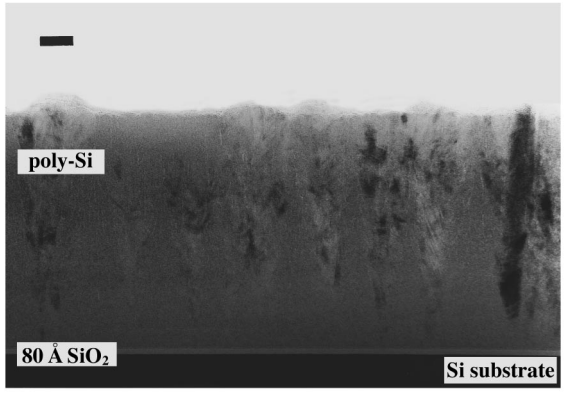

FIG. 11. Bright-field XTEM image of a two-stage film using epi-Si conditions ''A'' on an 80 Å μc-Si seed layer. The transition region consists of conically shaped crystalline Si grains separated by amorphous Si. The scale marker is 400 Å.

thickness upon bulk film crystallinity is examined. Figure 9 shows the Raman spectra for 2000 Å two-stage processed films using epi-Si conditions ''A'' on various μc-Si film thicknesses. Spectra are normalized to the 520 cm^{-1} peak height of the 80 Å μc-Si two-stage film for comparison. As seed layer thickness increases, the 480 cm^{-1} amorphous feature is shifted lower, indicating that the amorphous component in the films is decreasing. Note that two-stage processed films show the 520 cm^{-1} crystalline vibrational peak even for a seed layer thickness of only 5 Å. Also, although not shown, no 520 cm^{-1} peak was observed when a seed layer template was not deposited prior to bulk film growth.

Finally, for complete microstructural characterization, XRD and XTEM were performed on two-stage processed films incorporating an 80 Å μc-Si with epi-Si conditions ''A,'' i.e., films that showed the highest crystallinity as measured by RHEED and Raman spectroscopy. Figure 10 shows the XRD pattern for a 5000 Å thick film. In conjunction with the high intensity maximum seen at the zone center of the (220) ring in Fig. 5b, the XRD pattern shows that the two-stage films are highly (220) oriented. From structure factor calculations,[10] the (111) peak intensity should be approximately twice that of the (220) reflection for randomly oriented films. However, these films show a (220) reflection intensity that is significantly higher than that of the (111) peak, indicating a preferred orientation or texture. The use of simple surface free energy arguements, however, is not sufficient as an explanation of the texturing in the two-stage processed films. As mentioned previously, other complex factors associated with the microscopic geometry of the growing planes must be taken into account; these are reviewed in Ref. 7. XRD shows that not only can bulk film crystallinity be improved, but also that the orientation of the films can be controlled through interface engineering. Figure 11 shows a XTEM image obtained for the two-stage deposited films and illustrates why TEM must be used for complete microstructural analysis of the films. Crystalline grains are observed to nucleate at or near the μc-Si seed layer template (which is not distinguishable at this magnification) and grow in a cone-like fashion, with the grain size increasing as film growth proceeds. A transition layer extending from the oxide surface exists before grain coalescence occurs, i.e., the growing crystalline regions are separated by sections of amorphous material. No other characterization technique could reveal this. The growth rate of films deposited with and without a seed layer was approximately the same (~25 Å/min), adding no additional insight into why films deposited with a seed layer crystallized and those without did not. Further work is needed to explain these phenomena.

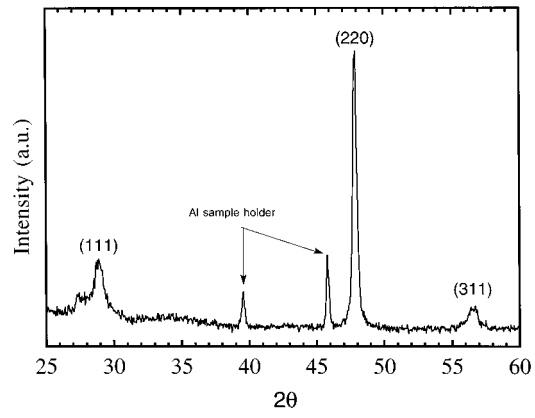

FIG. 10. X-ray diffraction pattern for a 5000 Å two-stage film using epi-Si conditions ''A'' on an 80 Å μc-Si seed layer.

IV. CONCLUSIONS

A low-temperature (<450 °C) plasma assisted CVD process that incorporates interface engineering has been demonstrated for growth of poly-Si thin films on SiO_2 and glass. Interface formation is separated from bulk film growth by employing two sets of process conditions. The first set, stage one, was optimized for depostion of ultrathin (<100 Å) μc-Si films on the oxide surface which act as a seed template for bulk film growth. Analysis on the growth of the μc-Si film was performed, and a layer type mechanism involving low-index crystal planes was suggested to explain the trends

in the data. Optimized conditions were then identified for producing low-temperature epitaxial silicon films on crystalline silicon substrates and were used as starting conditions for the second stage of film deposition to drive a transition to larger grain growth off of the seed crystals. Results indicated that when no seed template was used, the microstructure of films deposited using both sets of epi-Si conditions was amorphous. However, when a seed layer was deposited prior to bulk film depostion, highly (220) oriented poly-Si films could be obtained for one set of epi-Si conditions, while the other still produced amorphous films. The influence of seed layer thickness on crystallinity was examined and it was found that as seed layer thickness increases so does the bulk film crystallinity. Deposition of as little as a 5 Å thick μc-Si seed layer was shown to induce crystallinty in the bulk film. Cross-sectional TEM was used and it identified grains that nucleated at or near the seed layer and grow in a conelike fashion, with grain size increasing with film thickness. A transition region, however, extending from the oxide surface in which crystalline density was not maximized was noticed, i.e., the growing crystalline regions were separated by sections of amorphous material. Further work is needed to clarify directly how the seed layer influences growth of the second stage and to eliminate the transition region. In summary, it was shown that it is possible to drastically alter the bulk film microstructure of Si films on SiO_2 and glass by controlling interface formation.

ACKNOWLEDGMENTS

This work was supported by NSF, SRC, and ONR. The authors also thank B. Ward for his expertise in Raman spectroscopy and Dr. K. Christensen for the TEM imaging. This article is dedicated to John Reed.

[1]J. R. Heath, S. M. Gates, and C. A. Chess, Appl. Phys. Lett. **64**, 3569 (1994).
[2]A. Tanikawa and T. Tatsumi, J. Electrochem. Soc. **141**, 2848 (1994).
[3]T. Matsumoto, Y. Nagahiro, Y. Nasu, K. Oki, and M. Okabe, Appl. Phys. Lett. **65** 1549 (1994).
[4]G. Lucovsky, D. V. Tsu, R. A. Rudder, and R. J. Markunas, in *Thin Film Processes II*, edited by J. L Vossen and W. Kern (Academic, San Diego, 1991).
[5]M. Thompson, M. D. Baker, A. Christie, and J. F. Tyson, *Auger Electron Spectroscopy* (Wiley, New York, 1985).
[6]R. M. A. Azzam and N. M. Bashara, *Ellipsometry and Polarized Light* (North-Holland, Amsterdam, 1977).
[7]H. Kakinuma, J. Vac. Sci. Technol. A **13**, 2310 (1995).
[8]P. Bennema, in *Crystal Growth: An Introduction*, edited by P. Hartman (North-Holland, Amsterdam, 1973).
[9]Z. Iqbal, S. Veprek, A. P. Webb, and P. Capezzuto, Solid State Commun. **37**, 993 (1981).
[10]B. D. Cullity, *Elements of X-Ray Diffraction* (Addison-Wesley, Reading, MA, 1978).